Release of ADP from the catalytic subunit of protein kinase A: A molecular dynamics simulation study

BENZHUO LU,[1,2] CHUNG F. WONG,[3,4] AND J. ANDREW MCCAMMON[1–4]

[1]Department of Chemistry and Biochemistry, [2]Center for Theoretical Biological Physics,
[3]Department of Pharmacology, [4]Howard Hughes Medical Institute, University of California at San Diego,
La Jolla, California 92093-0365, USA

(RECEIVED May 27, 2004; FINAL REVISION August 25, 2004; ACCEPTED August 25, 2004)

Abstract

Substrate phosphorylation by cAMP-dependent-protein kinase A (protein kinase A, PKA) has been studied extensively. Phosphoryl transfer was found to be fast, whereas ADP release was found to be the slow, rate-limiting step. There is also evidence that ADP release may be preceded by a partially rate-limiting conformational change. However, the atomic details of the conformational change and the mode of ADP release are difficult to obtain experimentally. In this work, we studied ADP release from PKA by carrying out molecular dynamics simulations with different pulling forces applied to the ligand. The detailed ADP release pathway and the associated conformational changes were analyzed. The ADP release process was found to involve a swinging motion with the phosphate of ADP anchored to the Gly-rich loop, so that the more buried adenine base and ribose ring came out before the phosphate. In contrast to the common belief that a hinge-bending motion was responsible for the opening of the ligand-binding cleft, our simulations showed that the small lobe exhibited a large amplitude "rocking" motion when the ligand came out. The largest conformational change of the protein was observed at about the first quarter time point along the release pathway. Two prominent intermediate states were observed in the release process.

Keywords: ADP release; protein kinase A(PKA); hinge-bending motion; molecular dynamics pulling simulation

Protein phosphorylation is a very important regulatory mechanism in mammalian cells. Within the large and very diverse family of protein kinases, cAMP-dependent protein kinase (PKA), first characterized in 1968, (Walsh et al. 1968) is one of the most studied (Beebe and Corbin 1986; Taylor et al. 1990; Francis and Corbin 1994). The catalytic subunit of PKA has about 350 residues, with the conserved kinase core represented by residues 40–300 (Taylor et al. 1999). PKA was the first protein kinase discovered and purified (Walsh et al. 1968), sequenced (Shoji et al. 1979), and cloned, and expressed in large quantities in *Escherichia coli* (Slice and Taylor 1989).

Reprint requests to: J. Andrew McCammon, Department of Chemistry and Biochemistry, Center for Theoretical Biological Physics, Howard Hughes Medical Institute, University of California at San Diego, La Jolla, CA 92093-0365, USA; e-mail: blu@mccammon.ucsd.edu; fax: (858) 534-7042.

Article and publication date are at http://www.proteinscience.org/cgi/doi/10.1110/ps.04894605.

PKA serves as a molecular switch. One property that facilitates this is the flexibility of the protein. The crystal structures of the catalytic subunit with different ligands bound have revealed conformations that range from an open to a closed form, in which the N-terminal and C-terminal lobes are opened to different degrees (for review, see Johnson et al. 2001). The open form, which the apo protein adopts, may be important for ATP entrance or ADP release. The kinetics of the enzyme has also been studied experimentally, and the final step of ADP release was found to be rate-limiting (Grant and Adams 1996; Aimes et al. 2000; Adams 2003). Experiments such as small-angle X-ray scattering (Olah et al. 1993), stopped-flow measurements of ADP and ATP binding (Lew et al. 1997; Shaffer et al. 2001), catalytic trapping (Shaffer and Adams 1999), and hydrogen-deuterium exchange (Anderson et al. 2001; Hamuro et al. 2002) all suggested that conformational changes of the protein could play an important role in ligand

entry and release. However, the dynamical details of these structural changes are still unclear (Johnson et al. 2001).

Here, we describe molecular dynamics simulations that provide some insights into the mechanism of ADP release by PKA. The long timescale of ligand release presents a challenge to atomic-scale molecular dynamics simulations. The rate constant of ADP release is about $20s^{-1}$. This slow process is impossible to simulate with conventional MD simulations, which usually last no more than hundreds of nanoseconds. In this work, we accelerated the ADP release process by applying an external force to pull the ligand out. Analyzing the trajectories can give useful insights into the coupling between protein motion and ligand release.

Computational method and procedure

The dissociation of ADP from PKA is an energy barrier-crossing process whose kinetics may be described by the Arrhenius equation.

$$k_o = c\exp(-\beta\Delta G^{++}) \quad (1)$$

One can assume that an applied force lowers the energy barrier by an amount equal to the work that it performs, thus speeding up barrier crossing. The rate of passage over such a barrier under a constant force F may be approximated as

$$k(F) = k_o \exp(\beta F * x) \quad (2)$$

where x is the displacement from the stable-state energy minimum to the barrier peak along the reaction coordinate, which is parallel to the applied force. In our simulations, the applied force ranged in magnitude from 0.4 kcal/mol · Å to 1.5 kcal/mol · Å. These allowed the dissociation process to occur within the nanosecond time scale that is accessible to current all-atom molecular dynamics simulation technology.

System setup

We selected for our simulations a ternary complex structure (PDB code is 1JBP) containing the catalytic domain, ADP, and a 20-residue peptide substrate (Madhusudan et al. 1994). Since we focused on studying ADP release, which occurs after peptide release (see Fig. 6 in Madhusudan et al. 1994), we removed the peptide to form our simulation system. The n-octane in the PDB structure was also ignored. There are three phosphorylated residues (SEP10, SEP338, and TPO197) in the structure. A ribbon representation of the crystal structure and the applied force is shown in Figure 1A. Figure 1B shows the interaction of ADP with the C subunit in the crystal structure.

Simulation method

The MD simulation package NAMD was used in the force-pulling experiment (Kal et al. 1999), and the AMBER force field (Cornell et al. 1995; Meagher et al. 2003) was adopted. The complex was immersed in a rectangular box filled with TIP3P water molecules (Jorgensen et al. 1983). Hydrogens were added using the tool tleap in the AMBER package. The simulated system consisted of 342 residues, an ADP molecule, and 18,062 water molecules, making a total of

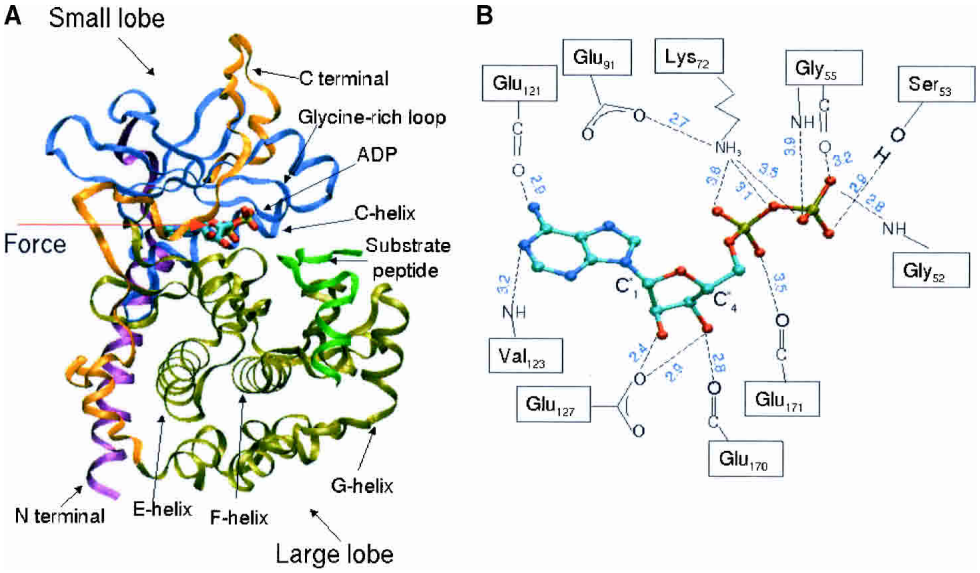

Figure 1. (*A*) The structure of the catalytic subunit of PKA and direction (red arrow) of the applied force in the simulation. ADP is shown in the stick representation. (*B*) Schematic diagram of the contacts between ADP and catalytic subunit. The distances are in Å.

59,846 atoms. The charges of the three phosphorylated residues were obtained by using Gaussian (6-31+G* basis set) together with the RESP method implemented in AMBER. The polyphosphate parameters for ADP were from the work of Meagher et al. (2003) developed for the force field of Cornell et al. (1995). The whole system was relaxed by energy minimization, then gradually heated from 0 to 300 K in 20 psec, followed by 800 psec of constant temperature equilibration at 300 K. The final structure was chosen for the following ADP release simulations.

We designed a set of pulling simulations with constant pulling forces of 1.5, 1.2, and from 1.0 to 0.4 kcal/mol · Å with 0.1 kcal/mol · Å decrements. We also performed the simulation with a pulling force equal to 0.3 kcal/mol · Å, but release did not occur within 30 nsec. The simulation with a pulling force equal to 0.4 kcal/mol · Å is denoted as F04; similar notations are used for other pulling forces. The forces were applied to the C_1^* atom that is in the ribose ring and connected to the adenine of ADP (see Fig. 1), (all atom names referred to in this article were those in the PDB file with code 1JBP). We chose the direction of the force to be parallel to the line connecting atom C_1^* of ADP and C_α of Glu 121, because this points to the entrance of the ADP pocket with relatively few possible bumps with the protein when the ligand is pulled out (see Fig. 1). We also carried out three other simulations by applying the external forces to different atoms or in different directions to examine whether the results changed significantly. In one, we used a different pulling direction (about 15° southeast away from the former one), pointing closer to the peptide-binding pocket. In the second one, we applied the force to atom C_4^* instead of C_1^* of ADP. Because atom C_4^* was closer to the phosphate group than C_1^*, this simulation was used to monitor whether the pulling position changed the release mode. In the third one, we carried out a steered MD (SMD) simulation, in which a harmonic constraint force (with a force constant of 1 kcal/mol · Å) was applied to the center of mass of the ligand to try to pull it out at a speed of 0.0002 Å/timestep. In all of the simulations, we fixed two atoms, Ala 147:CA and Gln 149:CA, in the protein, so that the ligand could be readily pulled out of the protein. Without fixing atoms on the protein, the protein tended to move together with the ligand. These two atoms were located in the rigid E helix of the protein kinase, and were far away from the ADP pocket and the active site, so as to minimize the effects of fixing them on the conformational changes observed in ligand release.

Langevin temperature control was used in all the simulations. The cut-off distance for nonbonded interaction was set to 10.0 Å, and a switching function beginning at 8.5 Å was used. All bonds were restrained to their equilibrium values by using SHAKE (Ryckaert et al. 1977). A 1-4 electrostatic interaction scaling factor of 0.83333 was used, and 1-4 VDW interactions were divided by a factor of 2.0.

Results and Discussion

Figure 2A shows the root mean square deviation (RMSD) of the complex structure from the crystal structure during the equilibration period. The RMSD was stabilized at about 2 Å. Figure 2B shows the RMSD of each residue of the final structure at the end of the equilibration run from the corresponding residue in the crystal structure. One can see that the G-helix shows a large displacement from its position in the crystal structure. Lowe et al. (1997) compared the binary complex (with ATP analog) and ternary complex (with ATP analog and a heptapeptide substrate) of the β-subunit of phosphorylase kinase (PHKβ), which resembles cAPK, and observed marked differences at the N terminus of the C-helix, the G-helix, and the C terminus. The temperature factors also indicated larger flexibility in these regions. They also noted that the differences in these regions might be related to the intermolecular contacts in the crystal. Large displacements of the G-helix were also observed in other protein kinases such as Csk (Hamuro et al. 2002). From hydrogen–deuterium exchange experiments, Hamuro et al.

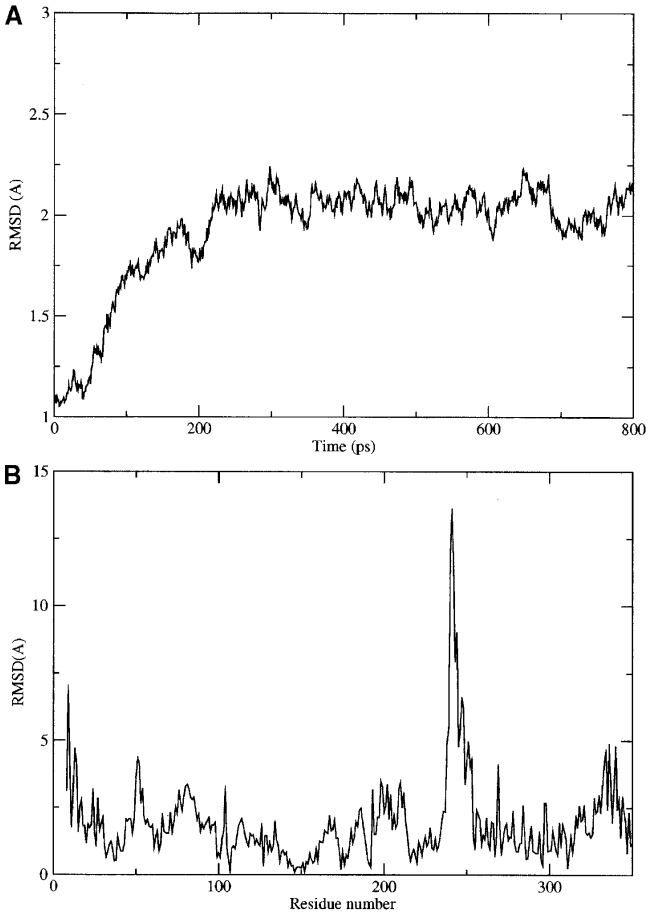

Figure 2. (*A*) RMSD (Å) of dynamics snapshots from the crystal structure during the equilibration period of the simulation. (*B*) Average RMSD (Å) of each residue of the structure after equilibration.

(2002) compared the exchange protections of the ATP-analog-bound and ADP-bound forms of the protein, and found large differences in the G-helix, suggesting large displacements of the helix when slightly different ligands were bound. Space-filling models illustrate that a peptide substrate packs closely against the preceding loop (residue 235–241) of helix G and part of the helix (Pro 243 and Ile 246 against Arg 374 of the peptide) in the crystal structure of the ternary complex. This suggests that the G-helix may act as a peptide recognition site and that peptide binding can mutually stabilize the G-helix and the peptide. The large conformational change observed in our simulation is likely due in part to the removal of the peptide from the crystal structure.

Mode of ADP release

Figure 3 shows the trajectory of the center of mass of ADP during the release process in simulation F04. We describe some characteristics in further detail below.

Forming and breaking of hydrogen bonds

The evolution of the hydrogen-bond network between ADP and the protein is illustrated in Figure 4 using snapshots from simulation F04.

In the first 160 psec of the simulation, the N_6 nitrogen in the adenine ring of ADP always hydrogen bonded to the backbone carbonyl oxygen of residue Glu 121 in the linker connecting the N-terminal and C-terminal lobes. Another strong hydrogen-bond network was found between the β-phosphate of ADP and the Gly-rich loop (such as Gly 55, Phe 54, Ser 53, Gly 52) of the protein. This hydrogen-bond network was maintained during the whole release process until ADP left the protein. At 180 psec, the hydrogen bond between the adenine ring and Glu 121 broke, and the adenine head flipped down a little in the binding pocket. This reorientation persisted for a long time until another hydrogen bond was formed between the ribose ring and residue Glu 127 in the linker region at 914 psec. From then on, the adenine head of ADP moved toward the intersection between Glu 127 and Glu 170, and formed hydrogen bonds with Glu 127(OE) and/or Glu 170(O). This state lasted for a long period from 914 to 2224 psec. As also supported by analysis to be provided below, this may be a primary intermediate state during ADP release. As shown in the figure, the β-phosphate always formed hydrogen bonds with the Gly-rich loop. In the final stage, the hydrogen bonds with Gly 55 and Gly 52 broke first, the one with Phe 54 broke next, and finally, the one with Ser 53(OH) disappeared at 2224 psec. This reveals the strongest interactions occurring between the β-phosphate of ADP and the Gly-rich loop of the protein.

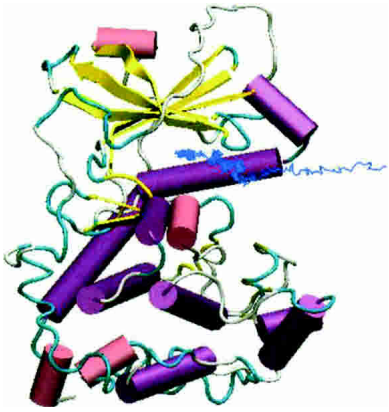

Figure 3. The trajectory (blue line) of the center of mass of ADP in the release simulation F04.

Also, the opening of the Gly-rich loop seemed essential to create some space for ADP release, as the adenine ring, which was further away from the opening than the phosphate group, came out first before the phosphate group released its grip with the Gly-rich loop, as described above. A short time later, after the breaking of the hydrogen bond between the adenine ring and Glu 170 at 2128 psec, followed by that between β-phosphate and Ser 53 at 2224 psec, the ADP left the binding pocket quickly. It is worth noting that in the simulation, the β-hydroxyl of Ser 53 also had a long-lasting hydrogen bond with the β-phosphate of ADP. This may explain why the S53G and S53P mutants released ADP faster than the wild type (see Table 3 in Aimes et al. 2000).

In addition to the hydrogen bonds between ADP and the Gly-rich loop, we also observed that Lys 72 interacted tightly with the α- and β-phosphates of ADP for a long time (the last H-bond contact broke at 1822 psec). The aromatic side chain of Phe 129 was found to turn outward to give way when the adenine moiety approached. It is worth noting here that all of these hydrogen-bond interactions with residues such as Glu 127, Glu 170, and Ser 53 may also affect the ATP-binding process, so that it is difficult to analyze the net effect of mutations on enzyme activity. The overall mechanism of PKA is a multiple-step process that involves substrate binding and dissociation, conformational changes, and chemical reaction. Therefore, even though a mutation may facilitate ADP release, it does not necessarily increase the enzyme activity. In fact, both the mutant E170A and the double-mutant E127A, P124A decrease the enzyme activity (Gibbs and Zoller 1991).

In summary, ADP release was found to occur like a swinging motion with the β-phosphate anchored to the Gly-rich loop. The adenine and the ribose ring swings from the less solvent-exposed side of the binding pocket to the solvent-exposed side of the pocket. This swinging motion also

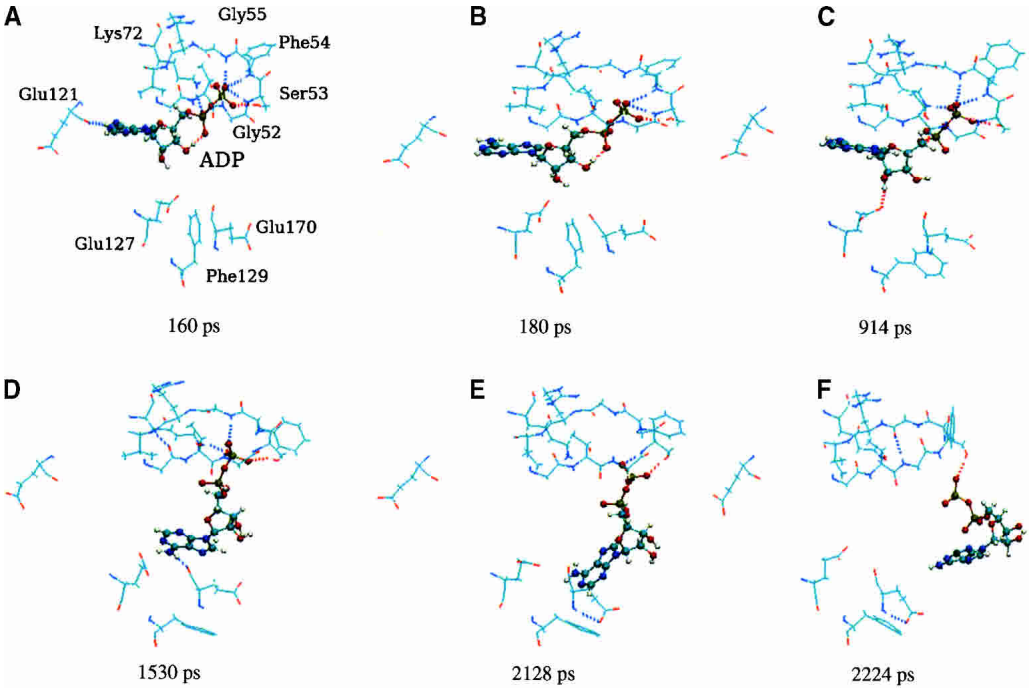

Figure 4. The evolution of the hydrogen bond network between ADP and PKA during ADP release in the F04 simulation.

occurred in all of the other simulations, including those with different force magnitudes, and those with different pulling force directions. This mode is also not altered in the simulation with the pulling force acting on atom C_4^*, which is closer to the phosphate group than atom C_1^*, supporting the picture of a strong interaction between the phosphate group and the Gly-rich loop. This general motion of ADP is likely to reflect what is actually happening in the enzyme. However, there were fine differences among the simulations. For example, we did not observe the insertion of the adenine ring into the area near Glu 127 and Glu 170 in the simulations with larger applied forces. The accompanying extensive stretching of ADP (see Fig. 4, 2128 psec) was also not found. In the cases with large applied forces, ADP left its binding pocket without large bending and stretching in the ribose ring. Figure 5, A and B (288 and 592 psec, respectively) show the simulation results with applied force equal to 0.5 kcal/mol · Å, in which ADP left smoothly without contacting Glu 170 after 592 psec. A possible reason is that the greater force allows the ADP to get over an energy barrier without forming the intermediate state. On the other hand, the results obtained from SMD, in which a constraint force was applied to the center-of-mass of the ligand, were more similar to the results obtained by applying a smaller force of 0.4 kcal/mol · Å. Again, ADP contacted the residues Glu 127 and Glu 170 during its release and it also adopted a stretched conformation (Fig. 5C,D). The similarity between the structural change observed in the SMD simulation and the one with a constant applied force of 0.4 kcal/mol · Å gives some confidence that the structural change observed in the simulations may reflect the actual ADP release process in the enzyme.

Conformational change of the protein

Dynamics of cleft opening and closing

The catalytic subunit of protein kinases contains a small C-terminal lobe and a larger N-terminal lobe (Taylor et al. 1999; Johnson et al. 2001). These two core domains, shared by all Ser/Thr and Tyr protein kinases, have different functional roles and dynamic characteristics (Smith et al. 1999). In general, the small lobe is more malleable and the large lobe is more structurally stable. The two lobes appear not to be tightly coupled, and the interactions between them are largely mediated by ligands such as ATP or ADP (Johnson et al. 2001). Opening of the cleft is likely essential for ADP release and ATP binding. Previous studies showed that the opening of the cleft was not a simple hinge movement, but a combination of hinging and sliding motions (Narayana et al. 1997; Tsigelny et al. 1999).

In the pulling simulations, we observed obvious hinge motion between the two domains. To characterize this motion by comparing dynamics snapshots with the crystal structure, we first moved each whole snapshot structure onto the crystal structure by superimposing the two more structurally stable large lobes, then checked the small lobes in the two structures to monitor the rotations. The Tcl script

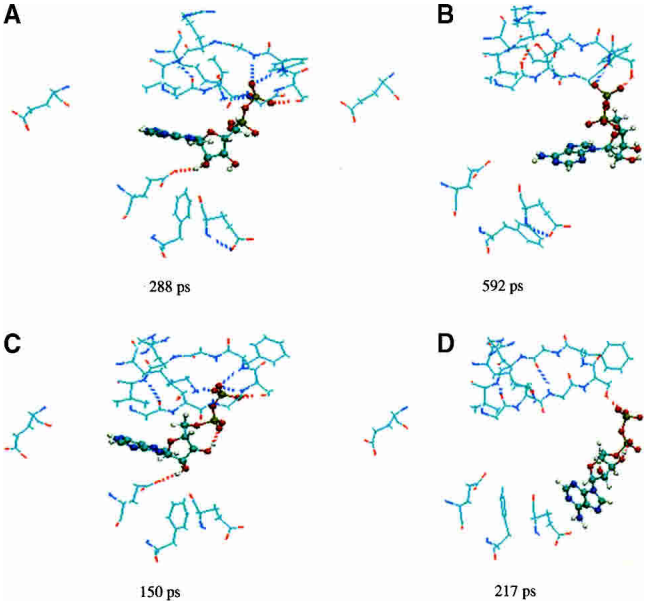

Figure 5. The evolution of hydrogen bond network between ADP and PKA during ADP release in the F05 and the steered MD simulations.

programming tool embedded in VMD (http://www.ks.uiuc.edu/Research/vmd/) was used to calculate and visualize the rotating motion. Any combined rotation and translation can be represented by operation of a 4 × 4 matrix on the moving object (see VMD manual), in which a 3 × 3 matrix formed by the first three columns and first three rows represents the rotation, and the fourth column is responsible for the translation. We carried out the following mathematical analysis to determine the rotation axis and angle. Suppose the two conformations were $\{x_S,x_L\}$ and $\{x'_S,x'_L\}$, where S and L denote the small and large lobes, respectively. First, a 4 × 4 matrix M_L was obtained by fitting the two large lobes. In other words, the new position x''_L ($= M_L x'_L$) of one large lobe was most similar to the other x_L in a least squares sense. Then, we applied the same operation M_L to the whole system such that $x''_L = M_L x'_L, x''_S = M_L x'_S$. The small lobe was then similarly fit to obtain another matrix M_S that made the new position $x'''_S = M_S x''_S$ least deviated from x_S. From the elements of a rotation matrix, one could calculate the rotation angle and the direction of the corresponding rotation axis defined by a unit vector. Together with the translational information in the 4 × 4 matrix, the location of the rotation axis (e.g., the hinge point) could be also determined. Then, we could obtain from the matrix M_S the rotation axis and angle that describe how the small lobe in one structure can be brought to the small lobe of another.

For each snapshot from the MD simulations, the rotation axis and rotation angle relative to the crystal structure were calculated. Figures 6 and 7 show the characteristics of the hinge motion. During the 20-psec warming-up simulation, in which the structure is still closed, it is found that the rotation axis varies a lot. This indicates that there is no well-defined hinge motion during this period, and the rotation angle was only <4° (Fig. 7A).

In contrast, in the equilibrium MD simulation prior to the force-pulling experiment, the different snapshots show small variation in the orientation of the rotation axis and in the position of the hinge point. This feature is kept in the ADP release simulation and another 2-nsec MD simulation after release of ADP (only the rotation angle of the last 500 psec as a function of time is shown in Fig. 7D). The average rotation axis for the ADP release process is shown in Figure 6A. The calculated rotation angle was in the range of 8° to 13° (Fig. 7B,D) in the MD simulations before and after ADP release. This is similar to the rotation angle calculated between "open" and "closed" pairs of crystal structures. This angle was 11° when calculated between the crystal structure with PDB code 1CTP (binary complex with diiodinated PKI, open conformation) and the crystal structure (PDB code 1JBP) used in the present simulation (Fig. 6B, red axis). It should be noted here that during relaxation after the substrate peptide was removed, the protein evolved into a rather open conformation and the pulling experiments started in this open conformation.

On the other hand, during the ADP release simulation, the rotation angle increased to as much as 19°. This suggests that larger thermal fluctuations are required when ADP goes through intermediate/transition states during its release. A detailed analysis of the time course of the rotation angle during ADP release (Fig. 7C) shows that domain opening started quickly after about 180 psec, when the hydrogen bond between adenine and Glu 121 broke (see Fig. 4). Following that, the rotation angle approached 19°, and this most-open conformation was visited again during the following 300-psec period, but not afterward. This observation, together with the results shown in the above section, indicates that the largest cleft opening occurred in the early stage of ADP release: when the adenine and ribose rings

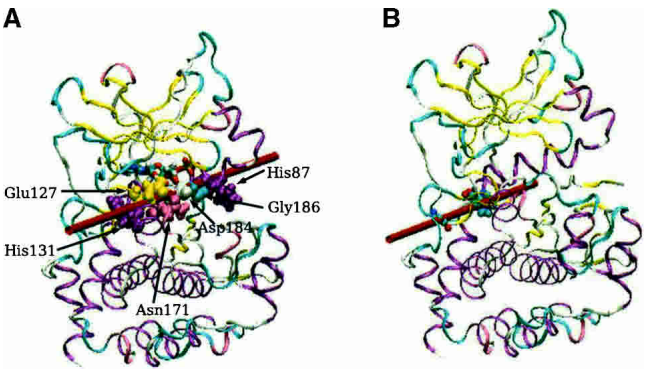

Figure 6. (*A*) Rotation axis averaged over the pulling simulation (red line). The residues that the axis passes through are shown in vdw spheres. (*B*) The rotation axis obtained by comparing the crystal structure 1JBP with an open form crystal structure 1CTP (red line).

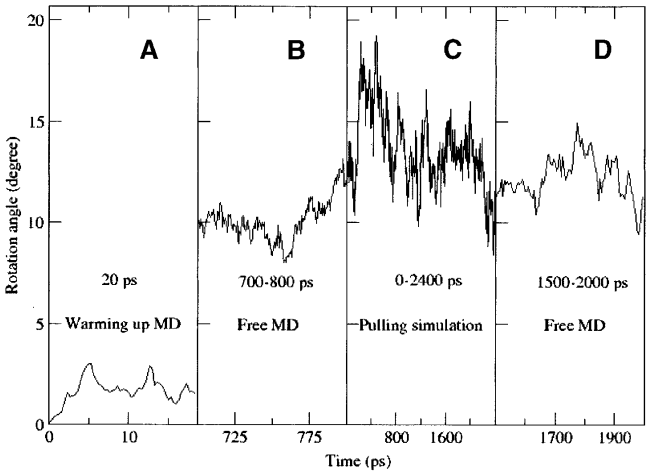

Figure 7. Rotation angles in different simulations. (*A*) The first 20 psec of the warming-up simulation, (*B*) from 700 to 800 psec of the free MD simulation prior to applying the pulling force, (*C*) the whole 2400 psec of the F04 simulation, (*D*) the last 500 psec in the 2-nsec free MD simulation after ADP was pulled out in the F04 simulation.

flipped out with the phosphate group still anchored to the Gly-rich loop. After ADP was released, at about 2200 psec, the two domains closed up by more than 4°, while still keeping an open conformation as in the apo form.

Kinetic experiments (Lew et al. 1997; Shaffer and Adams 1999; Shaffer et al. 2001) have been carried out to shed light on the ADP release mechanism. These experiments concluded that the rate-limiting step of ADP release might be partially controlled by conformational changes occurring after phosphoryl transfer, but before ADP release. The authors estimated that the rate of conformational change was 170 s^{-1} at a physiological magnesium concentration of 0.5 mM, and the ADP and peptide dissociation rate was about 140 s^{-1} (Scheme 2 in Shaffer and Adams 1999). Our pulling simulation suggests that the maximal protein conformational change is coupled tightly with the ADP release.

In addition to the rotation angle, the rotation axis was also determined for each snapshot. It is worth noting that the hinge point, through which the rotation axis passes, was somewhat different in our simulation from that suggested by previous workers based on qualitative structural analysis. It has often been assumed that the linker connecting the N-terminal and C-terminal lobes provides a hinge for the opening up of the ligand-binding pocket. In our simulation, the axis was displaced a bit away from the linker into the free space of the binding pocket. It passed a region surrounded by His 87, Glu 127, His 131, Asn 171, Asp 184, and Gly 186 (Fig. 6A). Glu 170 also flanks the axis (data not shown). Most of these residues (Glu 127, Glu 170, Asn 171, Asp 184, and Gly 186) form part of the ADP (ATP) binding pocket. As a result, the small lobe underwent a "rocking" motion with the rotation axis passing through the middle of the binding pocket.

When comparing the crystal structures between 1CTP and 1JBP, or between 1CTP and 1ATP, the rotation axis was found to pass through Val 98 (end of the C-helix), Leu 103 (αC-β4 loop), and Gly 178 (β8–β9 loop), which shows the difference between the hinge points in the MD pulling simulation and in the crystal-structure comparison. This location of the axis is somewhat underneath the linker from the view in Figure 6B, and a bit to the left of that for the pulling calculation. In the work of Olah et al. (1993), Gly 125 in the middle of the linker was used as the hinge point. On the other hand, our work did not presume where the hinge point or rotation axis was, and derived them from the mathematical prescriptions described earlier. The shift of hinge point to the middle of the ADP-binding pocket found in our simulation may reflect the coupling of ligand binding and the cleft vibration, because the ADP tends to glue the small lobe (Gly-rich loop) to parts of the large lobe as shown above. As suggested in the first hinge-bending calculation of McCammon et al. (1976), the motion of the protein could be significantly perturbed by the presence of substrate, so that detailed study requires taking the enzyme–substrate interaction into account.

In addition, the variation in the rotation axis obtained by analyzing different crystal structures also shows that the displacements are more complex than a simple hinge motion. This is partly due to structural fluctuations, and partly to the sliding motion of the small lobe relative to the large lobe (Narayana et al. 1997).

Structural fluctuations during ligand release

Figure 8 shows the structural deviations from the crystal structure for selected snapshots in the F04 and F05 simulations. The two snapshots in each simulation are one of a relatively closed conformation before ADP started to come out and one from the release process, respectively. The results illustrate which parts of the protein needed to adjust more in order for the ligand to come out. These include the Gly-rich loop and its sequential neighboring residues, the linker, the catalytic loop, the activation loop, the C terminus, the N terminus, and the G-helix. On the other hand, most helices in the large lobe, especially the E- and F-helices, were stable during the release process. Although the smaller overall displacements of the large lobe result in part from the superpositioning used in our analysis, the picture that emerges is that release of ADP requires sizable displacements of the small lobe and residues 318–350 of the C terminus relative to the core of the large lobe.

Most residues of the small lobe anchored C-terminal segment (from about residue 318 to 350) and the glycine-rich loop connecting β strands 1 and 2 move back toward the crystal structure when the ADP is completely off the kinase. It has been reported that the mobility of the glycine-rich loop on the small lobe and the C-terminal segment (residues

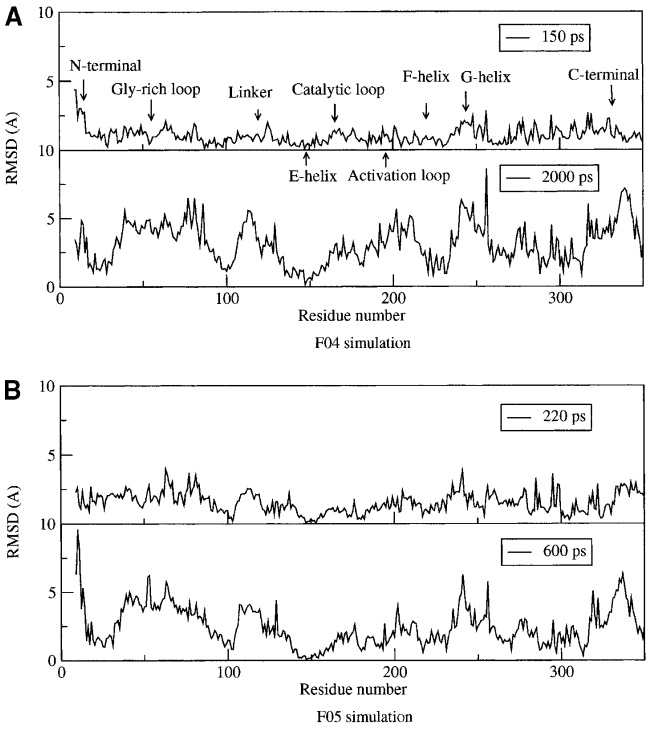

Figure 8. The RMSD of each residue from the crystal structure for selected dynamics snapshots, (*A*) at 150 and 2000 psec in the F04 simulation and (*B*) at 220 and 600 psec in the F05 simulation.

318–335) are all involved in contributing to nucleotide entry and exit from the active site (Narayana et al. 1997; Shaltiel et al. 1998), and the results of our simulation are consistent with this.

Kinetics study

Figure 9 shows the dissociation coordinate r_d as a function of simulation time in the forced release simulations. Figure 10 presents the occurrence frequency of r_d observed in simulations with different applied forces. The shortest dissociation time (when $r_d > 25$ Å) was found in simulation F15, in which the largest force was applied, and was < 40 psec. The longest dissociation time was found in simulation F04, in which the smallest force was applied, and was about 2300 psec. As the applied force was decreased, the intermediate states became more pronounced. As mentioned above, the larger forces may allow ADP to get over the energy barriers without forming or just briefly forming the intermediate states. The first intermediate state was found in the range 2–4 Å in most cases. The second one was found in the range of 5–10 Å. There were also subtle differences among the different simulations, indicating that the release pathway varied a bit from one simulation to the other. In the F04 simulation shown in Figure 10, the long-lived state in r_d 6–10 Å corresponded to the state in which the adenine end of ADP was displaced and tended to hydrogen bond with Glu 127 and Glu 170 (see Fig. 4). This simulation with the smallest applied force is likely closest to what is actually happening in the enzyme, and suggests a dissociation pathway characterized by two prominent intermediate states.

Conclusions

ADP release is the last step to complete kinase activity. Our simulation provided an atomistic view on how protein conformational changes might play a role in this dissociation process. In the simulation with the smallest applied force, simulation F04, the time for ADP to come out of the binding pocket was about 2300 psec. During this period, the largest rotation of the small lobe relative to the large lobe was about 19°. This angle then fell back to the normal rotation angle as seen in the ligand-free MD simulations (about 8°–13°). In

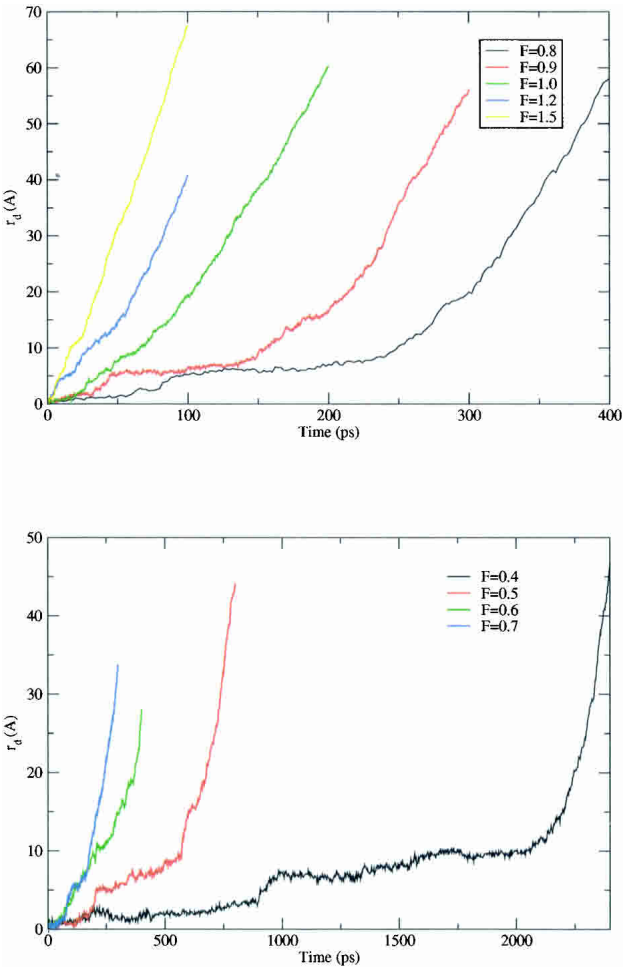

Figure 9. Time course of the ligand dissociation coordinate for the nine simulations with different pulling forces. The value in the legends following the character F is the pulling force in units of kcal/mol · Å.

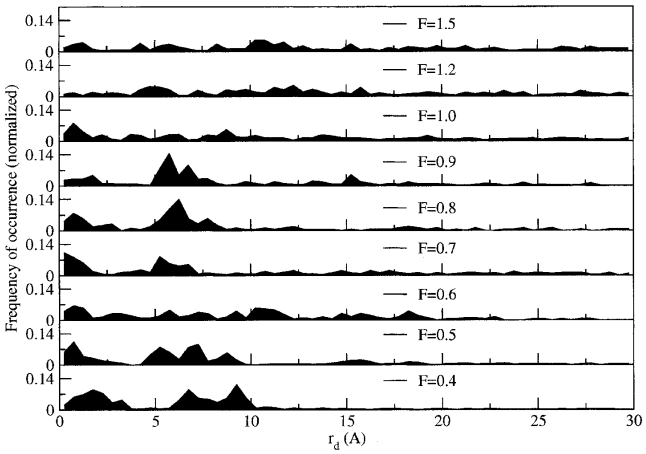

Figure 10. Normalized frequency of occurrence of the ligand dissociation coordinate for the nine simulations with different pulling forces.

the simulation, we also found that the rotation axis went through the ADP-binding pocket, rather than the linker connecting the N-terminal and C-terminal lobes. The opening of the cleft was thus achieved by a "rocking" motion of the small lobe with rotation axis displaced away from the linker region. The rotation of the small lobe appeared essential to facilitate ADP release, which was found to involve a swinging motion, in which the adenine base and the sugar ring first came out into the exterior, while the phosphate group was anchored onto the glycine-rich loop. The phosphate group then loosened its grip and the whole ADP molecule came out of the enzyme. In addition, our simulations suggested that the dissociation of ADP from the binding pocket might go through two intermediate states.

Acknowledgments

This work was supported in part by the NIH, NSF, the Howard Hughes Medical Institute, National Biomedical Computing Resource, the NSF Center for Theoretical Biological Physics, SDSC, the W.M. Keck Foundation, and Accelrys, Inc.

References

Adams, J.A. 2003. Activation loop phosphorylation and catalysis in protein kinases: Is there functional evidence for the autoinhibitor model. *Biochemistry* **42:** 601–607.

Aimes, R.T., Hemmer, W., and Taylor, S.S. 2000. Serine-53 at the tip of the glycine-rich loop of cAMP-dependent protein kinase: Role in catalysis, P-site specificity, and interaction with inhibitors. *Biochemistry* **39:** 8325–8332.

Anderson, M.D., Shaffer, J., Jennings, P.A., and Adams, J.A. 2001. Structural characterization of protein kinase A as a function of nucleotide binding: Hydrogen-deuterium exchange studies using MALDI-TOF MS detection. *J. Biol. Chem.* **276:** 14204–14211.

Beebe, S.J. and Corbin, J.D. 1986. *The enzyme: Control by phosphorylation Part A.* Academic Press, New York.

Cornell, W.D., Cieplak, P., Bayly, C.I., Gould, I.R., Merz, K.M., Ferguson, D.M., Spellmeyer, D.C., Fox, T., Caldwell, J.W., and Kollman, P.A. 1995. A 2nd generation force-field for the simulation of proteins, nucleic-acids, and organic-molecules. *J. Am. Chem. Soc.* **117:** 5179–5197.

Francis, S.H. and Corbin, J.D. 1994. Structure and function of cyclic nucleotide-dependent protein kinases. *Annu. Rev. Physiol.* **56:** 237–272.

Gibbs, C.S. and Zoller, M.J. 1991. Rational scanning mutagenesis of a protein-kinase identifies functional regions involved in catalysis and substrate interactions. *J. Biol. Chem.* **266:** 8923–8931.

Grant, B.D. and Adams, J.A. 1996. Pre-steady-state kinetic analysis of cAMP-dependent protein kinase using rapid quench flow techniques. *Biochemistry* **35:** 2022–2029.

Hamuro, Y., Wong, L., Shaffer, J., Kim, J.S., Stranz, D.D., Jennings, P.A., Woods Jr., V.L., and Adams, J.A. 2002. Phosphorylation driven motions in the COOH-terminal Src kinase, CSK, revealed through enhanced hydrogen-deuterium exchange and mass spectrometry (DXMS). *J. Mol. Biol.* **323:** 871–881.

Johnson, D.A., Akamine, P., Radzio-Andzelm, E., Madhusudan, and Taylor, S.S. 2001. Dynamics of cAMP-dependent protein kinase. *Chem. Rev.* **101:** 2243–2270.

Jorgensen, W.L., Chandrasekhar, J., Madura, J.D., Impey, R.W., and Klein, M.L. 1983. Comparison of simple potential functions for simulating liquid water. *J. Chem. Phys.* **79:** 926–935.

Kal, L., Skeel, R., Bhandarkar, M., Brunner, R., Gursoy, A., Krawetz, N., Phillips, J., Shinozaki, A., Varadarajan, K., and Schulten, K. 1999. Namd2: Greater scalability for parallel molecular dynamics. *J. Comp. Phys.* **151:** 283–312.

Lew, J., Taylor, S.S., and Adams, J.A. 1997. Identification of a partially rate-determining step in the catalytic mechanism of cAMP-dependent protein kinase: A transient kinetic study using stopped-flow fluorescence spectroscopy. *Biochemistry* **36:** 6717–6724.

Lowe, E.D., Noble, M.E.M., Skamnaki, V.T., Oikonomakos, N.G., Owen, D.J., and Johnson, L.N. 1997. The crystal structure of a phosphorylase kinase peptide substrate complex: Kinase substrate recognition. *EMBO J.* **16:** 6646–6658.

Madhusudan, Trafny, E.A., Xuong, N.H., Adams, J.A., Ten Eyck, L.F., Taylor, S.S., and Sowadski, J.M. 1994. cAMP-dependent protein-kinase: Crystallographic insights into substrate recognition and phosphotransfer. *Protein Sci.* **3:** 176–187.

McCammon, J.A., Gelin, B.R., Karplus, M., and Wolynes, P.G. 1976. Hinge-bending mode in lysozyme. *Nature* **262:** 325–326.

Meagher, K.L., Redman, L.T., and Carlson, H.A. 2003. Development of polyphosphate parameters for use with the AMBER force field. *J. Comput. Chem.* **24:** 1016–1025.

Narayana, N., Cox, S., Xuong, N.H., Ten Eyck, L.F., and Taylor, S.S. 1997. A binary complex of the catalytic subunit of cAMP-dependent protein kinase and adenosine further defines conformational flexibility. *Structure* **5:** 921–935.

Olah, G.A., Mitchell, R.D., Sosnick, T.R., Walsh, D.A., and Trewhella, J. 1993. Solution structure of the cAMP-dependent protein kinase catalytic subunit and its contraction upon binding the protein kinase inhibitor peptide. *Biochemistry* **32:** 3649–3657.

Ryckaert, J.P., Ciccotti, G., and Berendsen, H.J.C. 1977. Numerical-integration of cartesian equations of motion of a system with constraints—molecular-dynamics of n-alkanes. *J. Comput. Phys.* **23:** 327–341.

Shaffer, J. and Adams, J.A. 1999. Detection of conformational changes along the kinetic pathway of protein kinase A using a catalytic trapping technique. *Biochemistry* **38:** 12072–12079.

Shaltiel, S., Cox, S., and Taylor, S.S. 1998. Conserved water molecules contribute to the extensive network of interactions at the active site of protein kinase A. *Proc. Natl. Acad. Sci.* **95:** 484–491.

Shoji, S., Titani, K., Demaille, J.G., and Fischer, E.H. 1979. Sequence of 2 phosphorylated sites in the catalytic subunit of bovine cardiac-muscle adenosine 3′–5′-monophosphate-dependent protein-kinase. *J. Biol. Chem.* **254:** 6211–6214.

Slice, L.W. and Taylor, S.S. 1989. Expression of the catalytic subunit of cAMP-dependent protein-kinase in *Escherichia-coli*. *J. Biol. Chem.* **264:** 20940–20946.

Smith, C.M., Radzio-Andzelm, E., Madhusudan, Akamine, P., and Taylor, S.S.

1999. The catalytic subunit of cAMP-dependent protein kinase: Prototype for an extended network of communication. *Prog. Biophys. Mol. Biol.* **71:** 313–341.

Shaffer, G., Sun, J., and Adams, J.A. 2001. Nucleotide release and associated conformational changes regulate function in the COOH-Terminal Src kinase, Csk. *Biochemistry* **40:** 11149–11155.

Taylor, S.S., Buechler, J.A., and Yonemoto, W. 1990. cAMP-dependent protein kinase: Framework for a diverse family of regulatory enzymes. *Annu. Rev. Biochem.* **59:** 971–1005.

Taylor, S.S., Radzio-Andzelm, E., Madhusudan, Cheng, X.D., Ten Eyck, L.F., and Narayana, N. 1999. Catalytic subunit of cyclic AMP-dependent protein kinase: Structure and dynamics of the active site cleft. *Pharmacol. Ther.* **82:** 133–141.

Tsigelny, I., Greenberg, J.P., Cox, S., Nichols, W.L., Taylor, S.S., and Ten Eyck, L.F. 1999. 600 ps molecular dynamics reveals stable substructures and flexible hinge points in cAMP dependent protein kinase. *Biopolymers* **50:** 513–524.

Walsh, D.A., Perkins, J.P., and Krebs, E.G. 1968. An adenosine 3′,5′-monophosphatedependant protein kinase from rabbit skeletal muscle. *J. Biol. Chem.* **243:** 3763–3774.